IEICE TRANS. COMMUN., VOL.E92–B, NO.5 MAY 2009

PAPER

A Low-Complexity Minimum-Interference Symbol Time Estimation for OFDM Systems*

Wen-Long CHIN[†a)], ***Student Member and*** **Sau-Gee CHEN**[††], ***Member***

SUMMARY Conventional symbol time (ST) synchronization algorithms for orthogonal frequency-division multiplexing (OFDM) systems are mostly based on the maximum correlation result of the cyclic prefix. Due to the channel effect, the estimated ST is not accurate enough. Hence, one needs to further identify the channel impulse response (CIR) so as to obtain a better ST estimation. Overall, the required computational complexity is high because it involves time-domain (TD) correlation operations, as well as the fast Fourier transform (FFT) and inverse FFT (IFFT) operations. In this work, without the FFT/IFFT operations and the knowledge of CIR, a low-complexity TD ST estimation is proposed. We first characterize the frequency-domain (FD) interference effect. Based on the derivation, the new method locates the symbol boundary at the sampling point with the minimum interference in the FD (instead of the conventional maximum TD correlation result). Moreover, to reduce the computational complexity, the proposed FD minimum-interference (MI) metric is converted to a low-complexity TD metric by utilizing Parseval's theorem and the sampling theory. Simulation results exhibit good performance for the proposed algorithm in multipath fading channels.

key words: *OFDM, symbol time estimation*

1. Introduction

Orthogonal frequency-division multiplexing (OFDM) is a promising technology for broadband transmission due to its high spectrum efficiency, and its robustness to the effects of multipath fading channels. OFDM has been adopted by many state-of-the-art communication standards such as DVB-T, DAB, xDSL, WLAN systems based on 802.11x standards, and fixed or mobile MAN systems based on 802.16x standards. It has also become a key technology in mobile communication systems beyond 3G.

However, OFDM systems are sensitive to synchronization errors. First, unknown signal timing introduces the symbol time (ST) offset (STO), and require the ST synchronization. There also exists the carrier frequency offset (CFO) between a transmitter and receiver pair so that the fractional carrier frequency offset (FCFO), integral carrier frequency offset (ICFO) and residual carrier frequency offset (RCFO) have to be eliminated. In addition, the mismatch of sampling clocks between the DAC and ADC introduces the sampling clock frequency offset (SCFO).

The ST estimation is usually the first step in an entire OFDM synchronization process, because it provides an estimated OFDM symbol boundary for the remaining synchronization steps. For good ST estimation, one should consider the channel effects without introducing extra inter-symbol interference (ISI) and inter-carrier interference (ICI), and the signal-to-interference-and-noise ratio (SINR) is maximized.

In [1], the STO and FCFO are jointly estimated by a delayed-correlation algorithm. It is a maximum-likelihood (ML) estimation and only good for the additive white Gaussian noise (AWGN) channels. In [2], a new method making use of training symbols in time-domain (TD) is proposed. However, its correlation results exhibit a region of uncertainty in multipath fading channels [3]. A remedy for this ambiguity is proposed in [3]. Some techniques [2]–[5] produce good ST performances. However, these algorithms inherently search for the strongest path instead of the first one. Although the technique in [6] can identify the ISI-free region in multipath fading channels, for accurate ST estimation, it may involve many symbols. The work in [7] treats the ST in multipath fading channels. In [4] and [8], the channel frequency response (CFR) must be estimated first. The inverse fast Fourier transform (IFFT) is then applied to obtain the channel impulse response (CIR), which is then used to adjust the symbol boundary. The work in [9] is a frequency-domain (FD) non-data-aided (NDA) tracking technique for the ST estimation.

In summary, the above-mentioned methods are mostly based on the TD maximum cyclic-prefix (CP) correlation results combined with channel estimation to achieve satisfactory ST results. In this work, in order to obtain accurate ST estimation with low computational complexity, the proposed scheme is based on a new metric by minimizing interference in the FD. The combined interference due to ISI and ICI is applied to accurately locate the ST with the minimum interference. To reduce the computational complexity, the proposed FD minimum-interference (MI) metric is converted to a low-complexity TD metric by utilizing Parseval's theorem and the sampling theory. The proposed TD approach is low-complexity in the sense that knowledge of channel profiles and the FFT/IFFT operations are not required.

The rest of this paper is organized as follows. We

Manuscript received June 5, 2008.
Manuscript revised December 20, 2008.

[†]The author is with the Department of Engineering Science, National Cheng Kung University, Tainan 701, Taiwan, ROC.
[††]The author is with the Department of Electronics Engineering and Institute of Electronics, National Chiao Tung University, Hsinchu 30050, Taiwan, ROC.

*This work is supported in part by the grants NSC 95-2219-E-009-004 and MOEA 95-EC-17-A-01-S1-048, Taiwan.
This work was presented in part at the 33rd IEEE Int. Conf. Acoustics, Speech, Signal Processing (ICASSP'08), Las Vegas, USA, March 30–April 4, 2008.

a) E-mail: johnsonchin@pchome.com.tw

DOI: 10.1587/transcom.E92.B.1828

will introduce the OFDM system model in multipath fading channels in Sect. 2. The MI ST estimation is then detailed in Sect. 3. Simulation results are provided in Sect. 4. Finally, we conclude our work in Sect. 5.

2. OFDM System Model

A simplified OFDM system model is shown in Fig. 1. In the figure, $X_{l,k}/\tilde{X}_{l,k}$ is the transmitted/received FD data on the k-th subcarrier of the l-th symbol, $1/T_S$ is the sampling frequency, f_c is the carrier frequency, and $\hat{n}_\Delta$ is the estimated STO. On the transmitter side, N complex data symbols are modulated onto N subcarriers by using the IFFT. The last N_G IFFT samples are copied to the CP that is inserted at the beginning of each OFDM symbol. By inserting the CP, a guard interval is created so that ISI can be avoided and the orthogonality among subcarriers can be sustained. The receiver uses the fast Fourier transform (FFT) to demodulate received data.

As shown in Fig. 2, an estimated ST (associated with a STO n_Δ) generally falls into one of the three depicted regions: the Bad-ST1 region, the Good-ST region, and the Bad-ST2 region in which n_Δ is confined within the ranges of $-N_G \le n_\Delta \le -N_G + \tau_d - 1$, $-N_G + \tau_d \le n_\Delta \le 0$, and $1 \le n_\Delta \le N - 1$, respectively, where N_G is the length of the CP and τ_d is the maximum delay spread of the channel. Specifically, the Bad-ST1 and Good-ST (also known as ISI-free) regions are in the guard interval. When the ST is located in the Good-ST region, no ISI results; however when the ST is located in the Bad-ST1 and Bad-ST2 regions, the l-th symbol has ISI from the $(l-1)$-th symbol and the $(l+1)$-th symbol, respectively. Furthermore, the CFO and SCFO introduce additional ICI.

There is freedom to select the ST in the ISI-free region of the guard interval. This region is obviously defined by the channel length. The STO is with reference to the ideal ST of the l-th symbol, which is marked by the time index at zero in Fig. 2. Detailed analysis of the received FD data on the k-th subcarrier in these three regions can be found in [10], and the received FD data can be written as a general form below (for only the Bad-ST2 region)

$$\tilde{X}_{l,k} = \tilde{X}_{l,k}^{dsr} + \tilde{N}_k \tag{1}$$

where

$$\tilde{X}_{l,k}^{dsr} \triangleq \frac{N - n_\Delta}{N} H_k X_{l,k} W_N^{-kn_\Delta} \tag{2}$$

is the desired data, H_k is the CFR on the k-th subcarrier, and $W_N = e^{-j2\pi/N}$; and

$$\tilde{N}_k \triangleq \tilde{X}_{l,k}^{ici} + \tilde{X}_{l,k}^{isi} + v \tag{3}$$

is the combined interference plus the AWGN v, $\tilde{X}_{l,k}^{ici}$ and $\tilde{X}_{l,k}^{isi}$ are the ICI and ISI terms, respectively. Exact formula of $\tilde{X}_{l,k}^{ici}$ and $\tilde{X}_{l,k}^{isi}$ can be found in [10] and omitted here.

3. Proposed ST Estimation

3.1 Proposed Frequency-Domain Minimum-Interference (FD-MI) Estimation

Before introducing the proposed algorithm, we assume that in data transmission there are M uniformly-spaced pilot subcarriers in each OFDM symbol. Besides, the pilot values in different OFDM symbols are the same for the same pilot subcarrier index. Moreover, by assuming that the channel is quasi-stationary over two consecutive symbols, the received

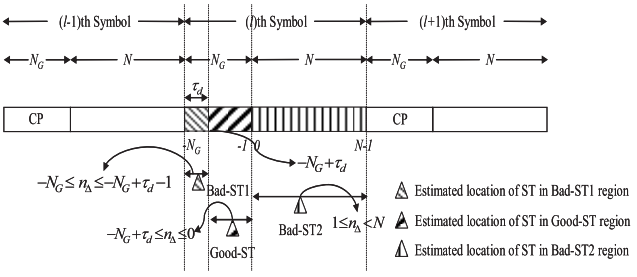

Fig. 2 Three different ST regions.

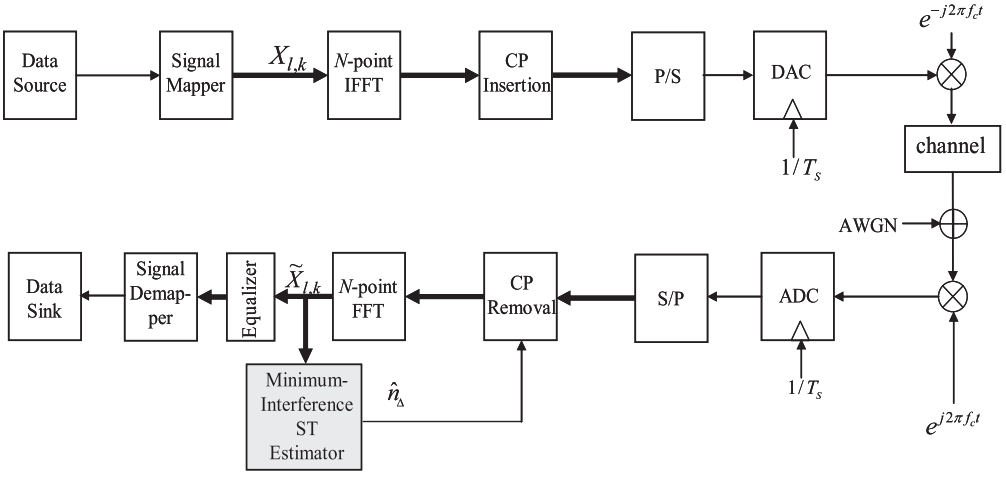

Fig. 1 A simplified OFDM system model.

pilot subcarriers will be the same in the ISI-free region because of nonexistence of the ISI and ICI. Otherwise, the received pilot subcarriers will be different in the Bad-ST1 and Bad-ST2 regions. By taking advantage of this property, we propose the following ST estimation metric

$$\hat{n}_\Delta = \arg\min_{n_\Delta} \sum_{k\in P} \left|\tilde{X}_{l+1,k} - \tilde{X}_{l,k}\right|^2,\ 0 \le n_\Delta < N_S \tag{4}$$

where P is the pilot set, and $N_S = N + N_G$ is the OFDM symbol length including the CP. Note that the dependence of $\tilde{X}_{l,k}$ on n_Δ is dropped for clarity. It will be shown in the following sectiton that the sampling point exhibiting the least value for the square-error sum (SES) metric in (4) is the MI symbol boundary in the Good-ST region.

3.2 Analysis of the FD-MI Estimation

From (1), since $\tilde{X}^{ici}_{l,k} = \tilde{X}^{isi}_{l,k} = 0$ in the Good-ST region, the expectation value of the SES metric in (4) in the Good-ST region can be easily shown to be

$$E\left[\sum_{k\in P}\left|\tilde{X}_{l+1,k} - \tilde{X}_{l,k}\right|^2\right] = 2M\sigma_v^2 \tag{5}$$

where σ_v^2 is the AWGN power. Likewise, the expectation value of the SES metric (4) in the Bad-ST2 region can be shown to be

$$\begin{aligned} &E\left[\sum_{k\in P}\left|\tilde{X}_{l+1,k} - \tilde{X}_{l,k}\right|^2\right] \\ &= \sum_{k\in P}\left\{E\left[\left|\tilde{X}^{ici}_{l+1,k} + \tilde{X}^{isi}_{l+1,k} - \tilde{X}^{ici}_{l,k} - \tilde{X}^{isi}_{l,k}\right|^2\right] + 2\sigma_v^2\right\} \\ &= \sum_{k\in P} E\left[\left|\tilde{X}^{ici}_{l+1,k} + \tilde{X}^{isi}_{l+1,k} - \tilde{X}^{ici}_{l,k} - \tilde{X}^{isi}_{l,k}\right|^2\right] + 2M\sigma_v^2 \\ &> 2M\sigma_v^2. \end{aligned} \tag{6}$$

The expectation value of the SES metric in the Bad-ST1 region can be similarly shown to be larger than that in the Good-ST region. From (5), (6), it is obvious that the SES metric (4) in the Good-ST region has the minimum value of only the AWGN power. Therefore, the proposed estimation locates the symbol boundary at the MI sampling point in the Good-ST region.

3.3 Proposed Low-Complexity Time-Domain Minimum-Interference (TD-MI) Estimation: The Frequency-Domain Counterpart

The computational complexity of the FD-MI in (4) is high because the pilot subcarrier responses must be derived for each sampling point. To reduce the complexity, one can transform (4) into a TD form by utilizing Parseval's theorem and the discrete-time Fourier transform (DTFT) sampling theory as follows.

It is assumed that the pilots are located at $\{0, \delta, \ldots, (M-1)\delta\}$, where $\delta = N/M$ is the pilot subcarrier spacing. Considering the DTFT of the received TD signal $\tilde{x}_{l,n}$

$$\tilde{X}_l(\omega) = \sum_{n=0}^{N-1} \tilde{x}_{l,n} e^{-j\omega n} \tag{7}$$

where n is the sample index and $0 \le \omega < 2\pi$. For each n_Δ, to obtain the pilot subcarrier responses, one needs to uniformly sample M data points of $\tilde{X}_l(\omega)$ at the pilot subcarrier frequency loications of $\omega_k = 2\pi k/N$, where $k \in P$ and $k = 0, \delta, \ldots, (M-1)\delta$. From the DTFT sampling theory, this results in the following sub-sampling of the DTFT (7)

$$\tilde{X}_{l,k'} = \sum_{n'=0}^{M-1} \widehat{x}_{l,n'} W_M^{k'n'},\ 0 \le k' < M \tag{8}$$

where k' is the sub-sampling index of k and $\widehat{x}_{l,n'}$ is the aliased version of $\tilde{x}_{l,n'}$.

$$\widehat{x}_{l,n'} = \sum_{i=0}^{\delta-1} \tilde{x}_{l,n'+iM},\ 0 \le n' < M. \tag{9}$$

Note that (8) is the discrete Fourier transform (DFT) of $\widehat{x}_{l,n'}$.

To find the optimum ST by using (4), assuming a specific ST n_Δ, we first need to compute the aliased TD signals $\widehat{x}_{l,n'}$ and $\widehat{x}_{l+1,n'}$ of $\tilde{x}_{l,n}$ and $\tilde{x}_{l+1,n}$, respectively, according to (9). Then, we calculate difference of the aliased sample as

$$\Delta\widehat{x}_{l+1,n'} \triangleq \widehat{x}_{l+1,n'} - \widehat{x}_{l,n'},\ 0 \le n' < M. \tag{10}$$

Finally, the metric (4) reduces to

$$\sum_{k\in P}\left|\tilde{X}_{l+1,k} - \tilde{X}_{l,k}\right|^2 = \sum_{k'=0}^{M-1}\left|\sum_{n'=0}^{M-1}\Delta\widehat{x}_{l+1,n'} W_M^{k'n'}\right|^2 \tag{11}$$

where $\sum_{n'=0}^{M-1}\Delta\widehat{x}_{l+1,n'} \cdot W_M^{k'n'},\ 0 \le k' < M$ can be realized by the FFT operation. The process is repeated for each n_Δ in the range of $0 \le n_\Delta < N_S$. As a result, it needs N_S FFTs to acquire pilot subcarriers.

To further reduce the huge amount of computation, we can utilize Parseval's theorem, and map the FD-MI estimation (4) into to the following TD-MI estimation

$$\begin{aligned} \hat{n}_\Delta &= \arg\min_{n_\Delta} \sum_{n'=0}^{M-1}\left|\widehat{x}_{l+1,n'} - \widehat{x}_{l,n'}\right|^2,\ 0 \le n_\Delta < N_S \\ &= \arg\min_{n_\Delta} \sum_{n'=0}^{M-1}\left|\Delta\widehat{x}_{l+1,n'}\right|^2,\ 0 \le n_\Delta < N_S. \end{aligned} \tag{12}$$

Note that the dependence of $\widehat{x}_{l,n'}$ on n_Δ is dropped for clarity. The metric can be averaged over symbols to enhance the estimation accuracy. Compared with conventional algorithms, the proposed TD-MI algorithm does not need to estimate the CIR and perform the FFT/IFFT operations.

The TD-MI estimation is summarized in the following steps. Note that the searched range covers a whole symbol duration (including the CP) of N_S samples.

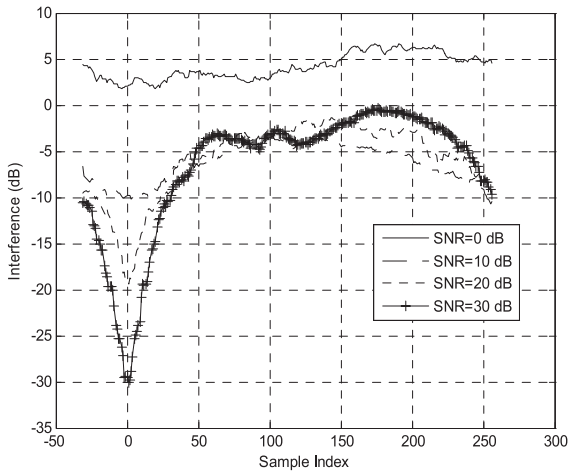

Fig. 3 Interference detected by the MI estimation of (12) against different sampling points.

Step 1: Initialize the minimum SES value (MinSES) to a enough-large value and denote i as the searched ST sampling index of n_Δ. For $i = 0$ to $N_S - 1$, do Step 2 to Step 3.

Step 2: Calculate the difference value, $\Delta\widehat{x}_{l+1,n'}$, $0 \le n' < M$, of the aliased samples, and the SES value $\sum_{n'=0}^{M-1} \left|\Delta\widehat{x}_{l+1,n'}\right|^2$ in (12).

Step 3: Compare the SES value with MinSES value and replace the MinSES value with the smaller value, i.e., MinSES=min$\{\sum_{n'=0}^{M-1} \left|\Delta\widehat{x}_{l+1,n'}\right|^2$, MinSES$\}$, where min{.} denote the minimum value function of its arguments. Store the MinSES value and its associated searched ST index i.

Step 4: The ST index i associated with the final MinSES is the estimated ST $\hat{n}_\Delta$.

3.4 Evaluation of the TD-MI Metric

The simulated SES metric of (12) under various signal-to-noise ratios (SNRs) is shown in Fig. 3. We assume an OFDM system of $N = 256$, $N_G = N/8 = 32$, and $M = N/32 = 8$ pilot subcarriers. The simulated modulation scheme is quadrature phase-shift keying (QPSK). The signal bandwidth is assumed to be 2.5 MHz and the radio frequency is 2.4 GHz. The subcarrier spacing is 8.68 kHz. The OFDM symbol duration is 115.2 μs. To verify the performance of the proposed technique, the channel is assumed to have N_G paths. Therefore, the Good-ST region contains only one sample (i.e., the 0th sample in Fig. 2). The channel taps are randomly generated by independent zero-mean unit-variance complex Gaussian variables with $\sum_\tau E\left\{|h_\tau|^2\right\} = 1$ for each simulation run, where h_τ is the channel coefficient of the τ-th path. In each simulation run, 10,000 OFDM symbols are tested. As can be seen, the metric has the minimum value in the Good-ST region (at the 0th sample).

Table 1 Comparison of computational complexities.

Methods	*No. of complex multiplications*	*No. of complex additions*
TD-MI	$N_SM/2$	$N_S(N+M-1)$
FD-MI [1]	$N_SNM/4$	N_SNM
TD-NDA1	N_SN_G	$N_S(N_G-1)$
TD-NDA2 [2]	$2N_S$	$\doteq 0$
MMSE	$3N_SN_G/2$	$N_S(3N_G-2)$
FD-NDA [3]	$\doteq N\left(\log_2 N + 1.5\right)$	$2N\log_2 N$

[1] The frequency-domain data are obtained by the Goertzel algorithm. Note that one real multiplication is counted as 1/4 complex multiplication and one real addition is counted as 1/2 complex addition.
[2] Besides complex multiplications, the TD-NDA2 also requires $2N_S$ square-root operations and N_S division operations.
[3] The radix-2 FFT is employed. Two FFT operations are required for received data of the early and late branches. Other operations are required for the metric.

3.5 Analysis of Computational Complexities of the Proposed Estimation and Conventional Techniques

The computational complexities of the proposed TD-MI and FD-MI estimations, and the conventional techniques such as the time-domain non-data-aided 1 (TD-NDA1) [1], the time-domain non-data-aided 2 (TD-NDA2) [6], the MMSE [7], and the frequency-domain non-data-aided (FD-NDA) [9] estimations are shown in Table 1. The searched range is within a window of N_S samples. Please note that, besides the complex multiplications of the TD-NDA2 listed in Table 1, the TD-NDA2 also requires $2N_S$ square-root operations and N_S division operations. Consequently, the TD-NDA2 is excluded from the following comparison.

For the proposed TD-MI estimation, within each searched index, $(N + M - 1)$ complex additions are needed, where the aliasing in (9) accounts for $N - M$ addition operations; and the subtraction and accumulation operations in (12) for M pilot subcarriers accounts for M and $M - 1$ addition operations, respectively. Since the squared magnitude of a complex number only costs two real multiplications and one addition, a squared magnitude operation is roughly counted as 0.5 complex multiplication. Therefore, within each searched index, $M/2$ complex multiplications are required in calculating the absolute-square of the interference.

Since the multiplication operation dominates the computational complexity, we focus on the comparison of the multiplication operation here. In comparison, for a system of $N = 256$, $M = N/32 = 8$, $N_G = N/8 = 32$, the required complex multiplications for the TD-MI, FD-MI, TD-NDA1, MMSE, and FD-NDA are 1,152, 147,456, 9,216, 13,824, and 2,432, respectively; and for a system of $N = 1024$, $M = N/32 = 32$, $N_G = N/8 = 128$, the required

complex multiplications for the TD-MI, FD-MI, TD-NDA1, MMSE, and FD-NDA become 18,432, 9,437,184, 147,456, 221,184, and 11,776, respectively. As can be seen, the computational complexity of the proposed FD-MI estimation is greatly reduced in its simplified TD-MI counterpart. In addition, the TD-MI requires the smallest number of multiplications when $N = 256$, while the FD-NDA requires the smallest number of multiplications, among the compared methods when $N = 1024$.

In summary, the computational complexity of the TD-MI is smaller than the FD-NDA for small N, but the result reverses for large N. Despite the comparable computational complexity, the TD-MI achieves better performance (in terms of the acquisition time and mean-squared error) than the FD-NDA as will be demonstrated in the next section.

4. Simulations

Monte Carlo simulations were conducted to evaluate the performance of the MI estimator in the above-mentioned OFDM system in Sect. 3.4. We evaluate the performance of the estimators by means of the estimators' normalized mean-squared error (MSE). All the results are obtained by averaging over 2,000 independent channel realizations.

4.1 Comparison among Different Methods

We compare the proposed estimation with the TD-NDA1 [1], TD-NDA2 [6], MMSE [7], and FD-NDA [9] techniques. In the FD-NDA, the time shift relative to the estimated symbol boundary for the early and late samples (that generate the S-curve) is assumed to be $N/4$. Besides, the loop bandwidth B_L is assumed to be 217 Hz. Regarding the tracking technique of the FD-NDA, it must be emphasized that there is no unique optimum design that can be applied in all conditions to the well-known compromise problem between the loop jitter and acquisition time [11], [12].

The performances of various algorithms are shown in Figs. 4 and 5. The estimated ST as a function of the symbol index at SNR = 15 dB is shown in Fig. 4. As can be seen, the estimated ST of the TD-MI estimator is accurately around the 0th sample. In addition, since the TD-MI estimator searches for the whole symbol duration, its acquisition time is short. In contrast, the FD-NDA is a tracking technique that has relatively longer acquisition time than the TD-MI. The acquisition time of the TD-NDA2 is also long because it has only one correlation result of neighboring symbols at each sampling point of a symbol. Therefore, the TD-NDA2 requires more symbols to achieve a satisfactory time-average result. The estimators' normalized MSE is shown in Fig. 5. As can be seen, the TD-MI exhibits lower MSE than the compared estimators except at the low SNR = 5 dB.

In summary, the MSE and the convergence time of the proposed TD-MI estimator are lower than those of the compared estimators.

4.2 Effect of Number of Pilot Subcarriers on Performance

We evaluate the system parameter such as the number of pilot subcarriers M on the proposed TD-MI estimator. The MSEs as a function of the SNR under various M are shown in Fig. 6. As can be seen, the MSE decreases when M increases, especially under low SNRs. However, under the conditions of SNR $\geq$ 25 dB or $M > 8$, the performance does not improve significantly.

5. Conclusion

In this work, a new ST estimation technique for OFDM systems is proposed and analyzed. The proposed technique has low-complexity properties: the knowledge of the channel profiles and the FFT/IFFT operations are not required; and the TD-MI estimation operates directly on the TD samples. It has been shown that the proposed technique acquires the ST with good accuracy in multipath fading channels.

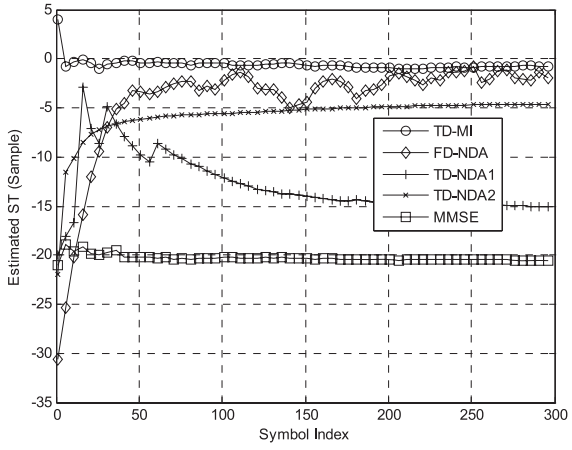

Fig. 4 Estimated ST against symbol index. SNR = 15 dB.

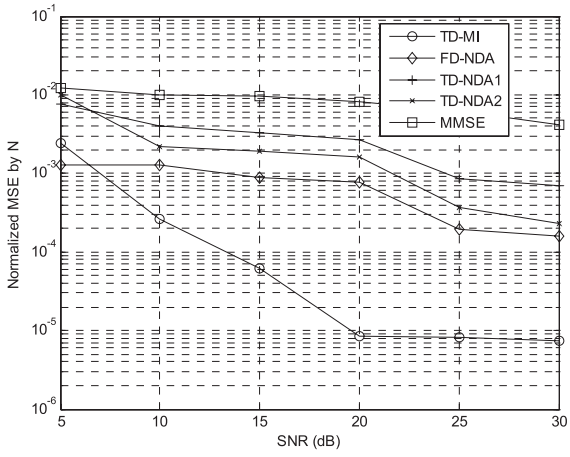

Fig. 5 Normalized MSE against SNR under various methods. $N = 256$. $M = 8$.

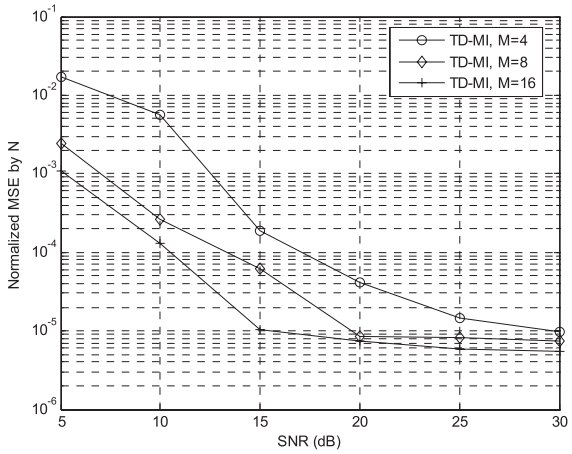

Fig. 6 Normalized MSE against SNR under various M. $N = 256$.

Acknowledgments

The authors would like to thank the Editor and anonymous reviewers for their helpful comments and suggestions in improving the quality of this paper.

References

[1] J.J. van de Beek, M. Sandell, and P.O. Börjesson, "ML estimation of time and frequency offset in OFDM systems," IEEE Trans. Signal Process., vol.45, no.7, pp.1800–1805, July 1997.
[2] T.M. Schmidl and D.C. Cox, "Robust frequency and timing synchronization for OFDM," IEEE Trans. Commun., vol.45, no.12, pp.1613–1621, Dec. 1997.
[3] B. Park, H. Cheon, C. Kang, and D. Hong, "A novel timing estimation method for OFDM systems," IEEE Commun. Lett., vol.7, no.5, pp.239–241, May 2003.
[4] H. Minn, V.K. Bhargava, and K.B. Letaief, "A robust timing and frequency synchronization for OFDM systems," IEEE Trans. Wireless Commun., vol.2, no.4, pp.822–839, July 2003.
[5] K. Shi and E. Serpedin, "Coarse frame and carrier synchronization of OFDM systems: A new metric and comparison," IEEE Trans. Wireless Commun., vol.3, no.4, pp.1271–1284, July 2004.
[6] K. Ramasubramanian and K. Baum, "An OFDM timing recovery scheme with inherent delay-spread estimation," GLOBECOM'01, IEEE, vol.5, pp.3111–3115, Nov. 2001.
[7] D. Lee and K. Cheun, "Coarse symbol synchronization algorithms for OFDM systems in multipath channels," IEEE Commun. Lett., vol.6, no.10, pp.446–448, Oct. 2002.
[8] M. Speth, S. Fechtel, G. Fock, and H. Meyer, "Optimum receiver design for OFDM-based broadband transmission-part II: A case study," IEEE Trans. Commun., vol.49, no.4, pp.571–578, April 2001.
[9] A.J. Al-Dweik, "A novel non-data-aided symbol timing recovery technique for OFDM systems," IEEE Trans. Commun., vol.54, no.1, pp.37–40, Jan. 2006.
[10] Y. Mostofi and D.C. Cox, "Mathematical analysis of the impact of timing synchronization errors on the performance of an OFDM system," IEEE Trans. Commun., vol.54, no.2, pp.226–230, Feb. 2006.
[11] A. Al-Dweik and R. El-Khazali, "A modified early-late gate for blind symbol timing recovery of OFDM systems," IEICE Trans. Commun., vol.E89-B, no.1, pp.11–18, Jan. 2006.
[12] F. Gardner, Phaselock Techniques, Wiley & Sons, NY, 1979.

Wen-Long Chin received his B.S. degree in electronics engineering from National Chiao Tung University, Hsinchu, Taiwan, in 1994, the M.S. degree in electrical engineering from National Taiwan University, Taipei, Taiwan, in 1996, and the Ph.D. degree in electronics engineering from National Chiao Tung University, Hsinchu, Taiwan, in 2008. In February 2009, he joined National Cheng Kung University, Taiwan, as an Assistant Professor. His research interests lie in the areas of (VLSI) signal processing, communications, and networks. Before holding the faculty position, he had worked in the Hsinchu Science Park, Taiwan, for over 11 years, all in charge of communication and network IC designs.

Sau-Gee Chen received the B.S. degree from National Tsing Hua University, Taiwan, in 1978, the M.S. degree and Ph.D. degree in electrical engineering, from the State University of New York at Buffalo, NY, in 1984 and 1988 respectively. During 2003 and 2006, he was Director of Institute of Electronics, Department of Electronics Engineering, National Chiao Tung University, Taiwan. Currently he is professor of the same organization. His research interests include digital communication, multi-media computing, digital signal processing, and VLSI signal processing. He has published more than 70 conference and journal papers, and holds several US and Taiwan patents.